

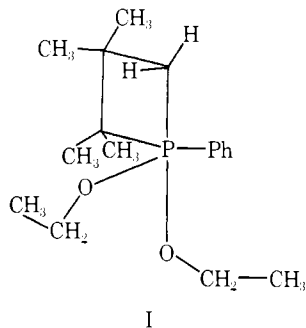
Structural Distortions of Cyclic Phosphoranes and the Berry Exchange Coordinate. A Quantitative Description¹

Robert R. Holmes* and Joan A. Deiters

Contribution from the Department of Chemistry, University of Massachusetts, Amherst, Massachusetts 01003. Received September 17, 1976

Abstract: Structural distortions of cyclic phosphoranes are shown to form a continuous series between the idealized trigonal bipyramidal (D_{3h}) and square pyramidal (C_{4v}) representations. The particular form of the distortions is along the Berry intramolecular exchange coordinate. Despite the lack of symmetry in the makeup of the cyclic substituents, a local C_{2v} constraint is closely followed. The origin of the mode of distortion is discussed in relation to the two sets of bond properties peculiar to five-coordinate geometries and the closeness in energy of the two idealized structures, enhanced by the presence of ring constraints. These findings reinforce the operation of successive Berry rearrangements postulated to account for NMR exchange data on a wide variety of phosphorane derivatives.

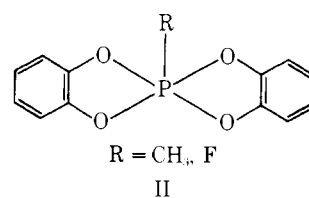
An intriguing problem in five-coordinate chemistry concerns the detailed reaction coordinate followed by nonrigid phosphoranes undergoing polytopal rearrangement. For many derivatives, successive ligand permutations are necessary to adequately account for NMR data obtained over wide temperature ranges.² The favored mechanism for ligand rearrangement is the Berry process.³ For example, the apparent equivalence of the methylene hydrogen atoms of the ethoxy groups observed⁴ in the ¹H NMR spectrum of I, obtained at 100 °C, is accountable by a minimum of five pseudorotations via the Berry mechanism in which each group bonded to phosphorus is used as a pivotal group.



In any particular Berry pseudorotation, intramolecular deformation is achieved by a concerted bending of axial and equatorial ligand pairs. A C_{2v} symmetry constraint is implied when all ligands are alike. The exchanging D_{3h} ground state structure passes through a square pyramidal intermediate (C_{4v}) on the way to the "pseudorotated" conformer (Figure 1).

For the example cited above (I), symmetry is lacking in the ground state representation and should bear some degree of structural deviation from the idealized trigonal bipyramid. As a consequence, there is no a priori reason to expect that the Berry exchange pathway ($D_{3h} = C_{4v} = D_{3h}$) should be closely followed. In fact, a permutationally equivalent exchange mechanism has been advanced,⁵ the turnstile process (Figure 2), which is governed by different symmetry conditions.

In theory, it should be possible to differentiate between mechanistic alternatives since different reaction coordinates are involved in each. In practice this has not been achieved. A possible approach is suggested by the recent characterization of cyclic phosphorane structures II by x-ray diffraction⁶ which more closely approximate an idealized square pyramid⁷ (the intermediate structural type in the Berry process), rather than the idealized trigonal bipyramid. By quantitative examination of structural distortions of a suitable series of phosphorane

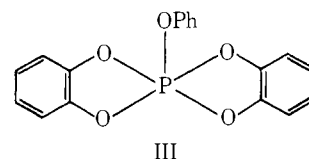


structures that extends incrementally from one idealized form to the other, and measurement of the magnitude that each individual structure deviates from a defined reaction coordinate, it may be possible to establish whether a preference for a particular pathway exists. In the subsequent presentation, two methods will be employed, one based on the measured angles at phosphorus and the other, first applied to five-coordinate complexes by Muetterties and Guggenberger,⁸ based on dihedral angles.

The purpose of the present paper is to show that application of the latter technique does indeed allow differentiation among exchange coordinates and leads to the Berry coordinate as the one governing structural deviations of cyclic phosphoranes. Succeeding papers⁹⁻¹¹ in this series refer to the structural elucidation of some key members that form the basis of the present interpretation.

Quantitative Assessment of Structural Distortions. Sum of Angles Method. Three basic structures are considered: the trigonal bipyramid (TP), the square pyramid (SP), and the turnstile representation (TR). Idealized geometries for these representations are shown in Figure 3. The square pyramid shown represents the barrier state in the Berry exchange mechanism³ while the 30° turnstile geometry is the barrier structure in the proposed⁵ turnstile exchange process.

In phosphoranes containing two five-membered rings, the observed internal ring angle at phosphorus is close to 90°. Hence, for these derivatives, a rectangular pyramid (RP) rather than a SP is a better representation of the barrier state in the Berry process. Angles for a 15° TR, representing a possible point along a turnstile exchange coordinate, are given in Figure 3 as well. The 15° TR geometry has been discussed as a preferred model for structural deviations of the catechol derivative III.¹²



As discussed in other articles⁹⁻¹¹ in this series, we have determined the molecular structures of a number of cyclic

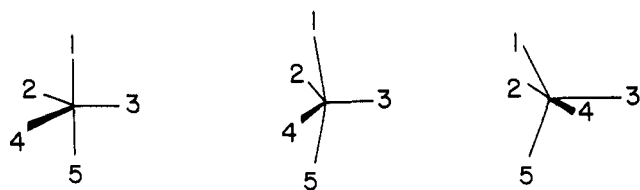


Figure 1. Berry exchange mechanism for the case involving all like ligands with position 3 as the pivotal ligand.

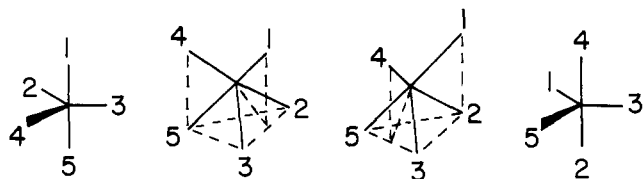


Figure 2. Turnstile exchange for MX_5 showing permutational equivalence with the Berry process (Figure 1). An equatorial in-plane bend decreases the angle 3–6–2 toward 90° , accompanied by a simultaneous rotation of atoms 4 and 1 relative to the other three atoms. Superimposed on these motions, atoms 4 and 1 also tilt them in equivalent positions relative to the triangular base atoms. The barrier structure is halfway between the two center structures shown here and is called a 30° TR.⁵

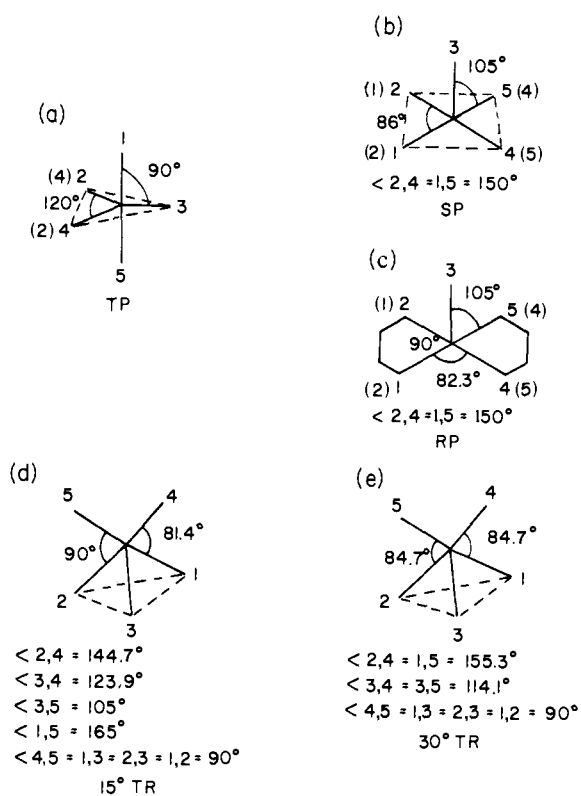


Figure 3. Idealized geometries: (a) trigonal bipyramid (TP); (b) square pyramid (SP); (c) rectangular pyramid (RP); (d) 15° turnstile (TR); (e) 30° turnstile (TR). The numbering scheme is not unique, although in representations (a)–(c) the only other possibility allowed is shown in parentheses which interchanges ligands only in the base planes.

phosphoranes by x-ray diffraction. Together with structural data on other cyclic derivatives which have appeared in the recent literature,^{6,12–16} including the first crystal structure of an oxyphosphorane^{15a} and x-ray parameters kindly supplied by Dr. W. S. Sheldrick^{17–21} on his interesting series of bicyclic and spiro phosphoranes, sufficient information is at hand to critically examine the magnitude and direction of structural deviations from idealized representations given in Figure 3. The structures that will concern us are depicted in Figure 4

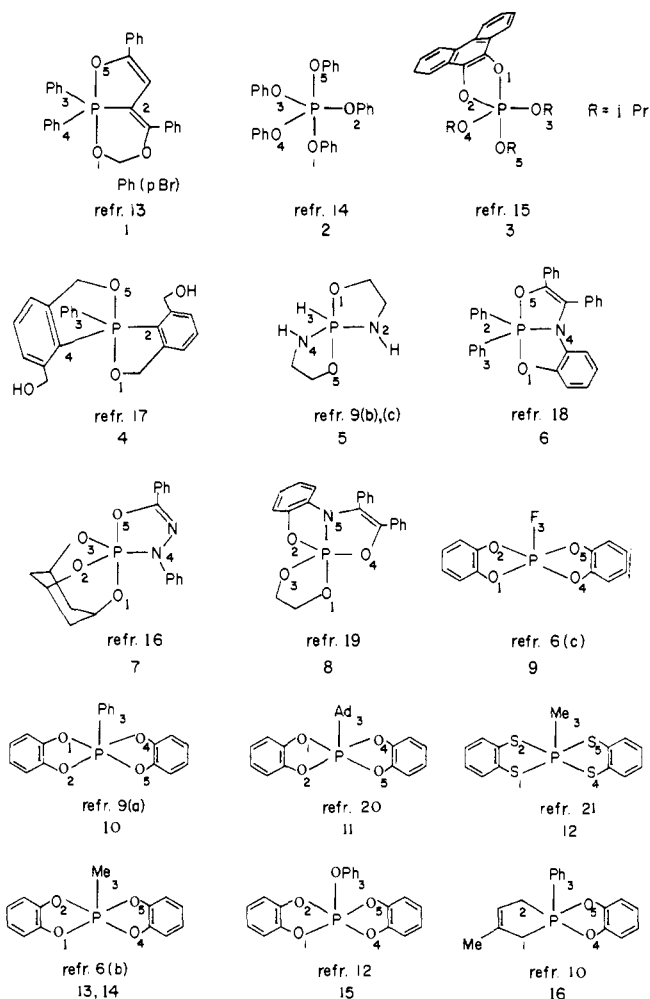


Figure 4. Compound number identification of structures referred to in Tables I, II, and III. In all of these structures ligands 2, 3, and 4 are oriented equatorial in a (TP) frame. In a SP or RP representation, ligand 3 is the axial ligand and ligands 2 and 4 have residual equatorial TP character. All the structures show distortions from idealized representations. They are given here in a form closest to one of the idealized representations. To redraw the structures in terms of other idealized representations, use this ligand numbering scheme relative to that shown in Figure 3. The best 30° TR structures are obtained from the ligand numbering and reference to Figure 3(e) except for entries 3 and 15. See footnote *a* to Table I for these derivatives. For entry 11, Ad = adamantyl. For entry 7, the x-ray structure^{16b} of the related compound with a $C(CF_3)_2$ group in place of the equatorial N–Ph group shows very similar bond parameters. The ligand numbering is the same as shown here for 7 except for the interchange of 2 and 3. The dihedral angle method (cf. Table III) shows the structure displaced 34% along the Berry coordinate toward the SP.

along with literature references. The caption for Figure 4 indicates the ligand numbering which determines the specific connecting idealized representations for each derivative as referenced in Figure 3.

The results on these cyclic pentacoordinate phosphorus compounds are summarized in Table I. For each compound designated in column 1, the sum of the observed angle deviations from each of the idealized structures, the TP, SP (or RP if two five-membered rings are present), the 15° TR, and the 30° TR configuration, is listed in columns 2, 3, 7, and 10, respectively. The sum represents the deviations of the ten angles involving the phosphorus atom in each of the structures.

It matters which ligand is taken as the single axial atom in the SP (RP), or which set of atoms forms the pair in the TR configuration, for purposes of calculating structural deviations. For all derivatives, various possibilities were examined, if not obvious, to define the ligands in such a way that the minimum

Table I. Structural Distortions of Cyclic Phosphoranes Based on the Sum of the Angles at Phosphorus, deg

1 Entry ^a	2 $\Sigma_i \theta_i(C) - \theta_i(TP) = A^b$	3 $\Sigma_i \theta_i(C) - \theta_i(SP) = B^c$	4 $S - B = A^*d$	5 $A + A^*/2$	6 $ A - A^* ^e$	7 ^f $\Sigma_i \theta_i(C) - \theta_i(15^\circ TR) = C$	8 $T' - C^g = A'$	9 $ A - A' ^h$	10 ^f $\Sigma_i \theta_i(C) - \theta_i(30^\circ TR) = D$	11 $T'' - D^g = A''$	12 $ A - A'' ^i$
1	23.7	130.1	5.9	14.8	17.8	104.9	-7.7	31.4	126.5	4.1	19.6
2	24.4	115.8	20.2	22.3	4.2	95.8	1.4	23.0	121.4	9.2	15.2
3	31.1	113.1	22.9	27.0	8.2	88.3	8.9	22.2	109.7 ^a	20.9	10.2
4	37.7	110.1 (RP)	25.3	31.5	12.4	87.7	9.5	28.2	109.3	21.3	16.4
5	34.1	110.5 (RP)	24.9	29.5	9.2	87.1	10.1	24.0	108.7	21.9	12.2
6	44.4	91.6	44.4	44.4	0.0	75.0	22.2	22.2	106.6	24.0	25.0
7	65.4	96.6	39.4	52.4	26.0	82.4	14.8	50.6	101.5	29.1	36.3
8	49.0	87.0	49.0	49.0	0.0	86.2	11.0	38.0	100.2	30.4	14.0
9	88.5	44.7 (RP)	90.7	89.6	2.2	77.1	20.1	68.4	85.3	45.3	43.2
10	102.7	32.7 (RP)	103.3	103.0	0.6	60.7	36.5	66.2	61.7	68.9	33.8
11	108.0	28.6 (RP)	106.8	107.4	1.2	66.8	30.4	77.6	63.8	66.8	41.2
12	108.7	32.9 (RP)	102.5	105.6	6.2	65.3	31.9	76.8	68.9	61.7	47.0
14	117.2	20.6 (RP)	114.8	116.0	2.4	69.8	27.4	89.8	61.6	69.0	48.2
15	120.3	29.6 (RP)	105.8	113.1	14.5	74.7	22.5	97.8	61.9 ^a	68.7	51.6
16	118.8	32.2 (RP)	103.2	111.0	15.6	64.6	32.6	86.2	70.0	60.6	58.2

^a Refer to Figure 4 for the phosphorane formula corresponding to the entry number. The ligand positioning of each entry for comparison with the idealized TP and SP (RP) structures is identified in Figure 4. For comparison with the idealized 15° TR and 30° TR of Figure 3, the ligand numbering in Figure 4 gives the best representation except for those value entries in column 10 indicated by a superscript (a). For entries 3 and 15, the best 30° TR representation is obtained by numbering the triad 543 instead of 123 indicated in Figure 3 (e) and 21 for the ligand pair instead of 45. ^b The sum of the absolute values of the differences of the ten observed angles at phosphorus for a specific phosphorane and the respective angles at phosphorus in the idealized TP (Figure 3 (a)). ^c Calculated as in b, except referenced to the idealized SP or RP depicted in Figure 3 (b) and (c), respectively. When the RP is the reference structure, it is indicated in parentheses in this column. ^d The symbol *S* indicates the value of the sum as defined in b when this sum is taken between the idealized TP and either the SP or RP (depicted in Figure 3 (a)–(c)). When the SP is used, *S* = 136°, when the RP is used, *S* = 135.4°. Thus, columns 2 and 4 are referenced from the TP end of the scale (with the TP end being 0°). If a Berry coordinate is strictly followed for structural distortions, columns 2 and 4 should have the same value for a specific entry. ^e The difference in absolute value between columns 2 and 4. A measure of the structural deviation from the Berry coordinate. ^f The data in columns 7–9 and 10–12 are calculated similarly to that discussed for columns 3, 4, and 6 in footnotes c, d, and e. Columns 7–9 refer to the 15° TR shown in Figure 3 (d) while columns 10–12 refer to the 30° TR (Figure 3 (e)). ^g The angle sum as defined in b when the sum is taken between the idealized TP and either the 15° TR (T') or 30° TR (T''). For the 15° TR, T' = 97.2°; for the 30° TR, T'' = 130.6°. ^h The difference in absolute value between columns 2 and 8 as a measurement of the extent to which structures distort from an idealized TP to a 15° TR. ⁱ The difference in absolute value between columns 2 and 11 as a measure of the extent to which structures distort from an idealized TP to a 30° TR.

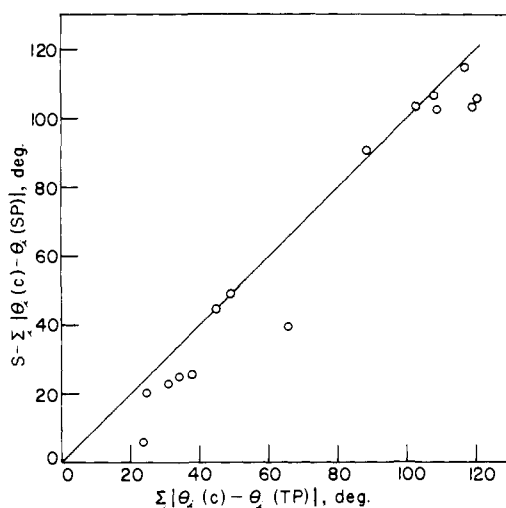


Figure 5. Cyclic phosphoranes showing distortion along the Berry exchange coordinate (solid line). The ordinate represents the sum of angular distortions of each compound from an idealized SP (RP) referenced to the same scale as used for the abscissa, $S - \Sigma_i |\theta_i(C) - \theta_i(SP)|$. The abscissa represents the sum of angular distortions for each compound from an idealized TP, $\Sigma_i |\theta_i(C) - \theta_i(TP)|$.

sum of angular deviations from the idealized SP (RP) and TR representations is obtained. This was particularly important for ligand definitions relative to the idealized turnstile geometries shown in Figure 3.

Since the sum of the ten angular changes encountered on going from the TP to the SP geometry is 136° (135.4° for the RP), the values in column 3 are subtracted from 136° (or 135.4° for the RP representation) to obtain the values listed in column 4. In other words, if structural distortions follow a

Berry coordinate, the values in columns 2 and 4, which are now both referenced as distortion sets with the idealized TP as 0°, should be the same. The extent to which they individually deviate is shown in column 6.²² For comparisons among the various derivatives, an average value of structural distortion (average of columns 2 and 4) is given in column 5.

Considering the variety of ground state structures with their lack of symmetry, individual ring strain, and steric effects, it is remarkable that the structural distortions follow the Berry exchange coordinate so closely. This correspondence is shown in Figure 5 where the angular distortions summed from each of the two idealized geometries, the TP and SP (RP), are plotted against each other (column 4 vs. column 2).

In contrast, a similar comparison for the turnstile pathway, that was illustrated in Figure 2, shows little correspondence between the angular deviations summed from the TP and TR geometries (cf. columns 2 and 8 of Table I for the 15° TR and columns 2 and 11 for the 30° TR). The reference value, the idealized TP structure taken as 0°, is the same for these comparisons as was used for the Berry pathway. In the calculation of the values in columns 8 and 11, the angular distortions summed from the 15 and 30° TR geometries (Figure 3) are subtracted from 97.2 and 130.6°, respectively. The latter values are the total angular changes over the ten phosphorus angles that take place on converting the idealized TP to the respective 15 and 30° TR configurations.

The data in columns 9 and 12 are instructive in that they show that as the observed structures distort away from the TP geometry toward the SP (RP) under the C_{2v} constraint of the Berry coordinate, the deviations from either turnstile geometry, in general, progressively increase. Furthermore, although the 15° TR, in general, gives a lower sum for the angular deviations about phosphorus compared to that for the 30° TR geometry (cf. columns 7 and 10), the 30° TR shows lower de-

Table II. Variation of the Dihedral Angle δ_{24} with the Angles θ_{15} and θ_{24} at Phosphorus, deg^a

Entry ^b	δ_{24}	θ_{15}	θ_{24}
1	53.1	176.9	124.0
4	44.2	178.1	133.9
2	43.9	176.6	125.5
3	42.6	175.2	125.5
5	41.0	177.0	131.7
6	39.9	171.6	130.6
7	38.9	169.8	129.5
8	34.5	172.4	134.0
9	22.2	168.2	146.1
10	14.2	160.0	145.4
12	14.0	158.0	143.5
11	12.1	157.1	144.1
15	8.7	160.0	151.4
13	8.5	156.2	147.7
14	8.4	156.9	148.1
16	2.6	152.5	150.0

^a With reference to Figure 3(a)–(c), the dihedral angle δ_{24} goes to zero as the Berry coordinate is traversed with ligand 3 as the pivotal ligand. The angles θ_{15} and θ_{24} at phosphorus then become trans basal angles in the SP (RP) representation. ^b Formula identification is given in Figure 4. Entries 13 and 14 are for the same compound which exhibits two slightly different structures in the unit cell. Structure I of ref 6b is labeled 14 here and structure II of ref 6b is entry 13.

viations referenced to a TP scale than does the 15° TR geometry (cf. columns 12 and 9).

Dihedral Angle Method. Perhaps a better method representing structural distortions is to calculate dihedral angles between triangular faces as outlined by Muetterties and Guggenberger⁸ and examine these relative to the idealized TP and SP (RP) structures. If the calculation is performed using all observed angles and distances rather than only unit distances,⁸ it is possible to evaluate the full effect of structural distortions. For example, as the structural distortion toward a SP occurs, the bond lengths as well as the bond angles show evidence of residual TP character. The longer pair of bond lengths when like ligands are involved is associated with the larger trans basal angle of a SP (RP), indicative of the axial character of the TP, while the shorter pair of bond lengths is associated with the smaller trans basal angle, indicative of residual equatorial TP character (see references indicated in Figure 4 for structural parameters of compound entries 2, 3, 7–15).

In a manner analogous to that of Muetterties and Guggenberger,⁸ a plot of each trans basal angle, or what would be a trans basal angle if a SP were formed (angles 24 and 15 with reference to the ligand definitions given in Figure 3), vs. the dihedral angle δ_{24} undergoing the greatest change on going from the TP to the SP (RP) geometry, i.e., from 53.1° to 0°, is shown in Figure 6. The latter angle δ_{24} is that formed between normals to the TP faces, 124 and 245, which faces have the common equatorial edge 24 (Figure 3(a)). This edge disappears in a SP or RP having four equal basal bond distances; thus, the dihedral angle becomes 0°. The corresponding data used in constructing Figure 6 are summarized in Table II.

The set of dihedral angles for each cyclic phosphorane is listed in Table III.²³ If we compare each dihedral angle for a specific compound with the corresponding values for the idealized TP and SP (RP) geometries and take these differences, we may compare the sum of the differences for each set on a common scale as was done for the sum of the ten angular deviations around phosphorus as discussed for Table I. The results of the new comparison are included in Table III. The scale is provided by the sum of the respective dihedral angle changes between the TP and SP (RP) geometries. This value is 217.9°

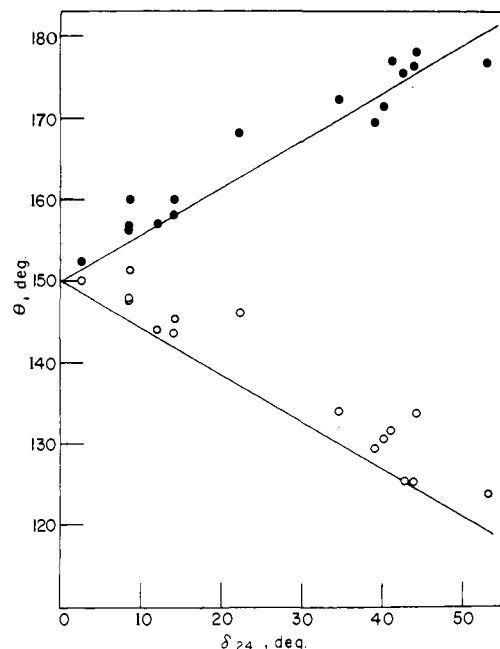


Figure 6. Variation of the angles at phosphorus θ_{15} (filled circles) and θ_{24} (open circles) vs. the dihedral angle δ_{24} as structural distortion proceeds along the Berry coordinate (solid lines) from a SP (RP) toward a TP.

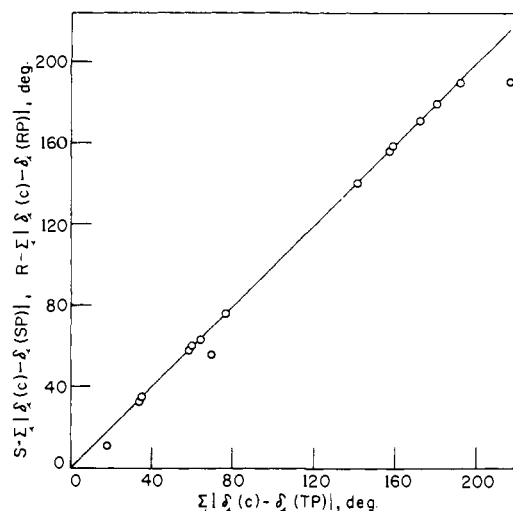


Figure 7. The sum of dihedral angles for cyclic phosphoranones from a SP (RP) idealized geometry vs. that from a TP geometry on a common reference scale. The solid line is along the Berry exchange coordinate. The point for structure 16 (farthest to the right) is off the line no doubt because of the presence of lattice disorder.¹⁰

for $\sum_i |\delta_i(\text{TP}) - \delta_i(\text{SP})|$ and 217.7° for $\sum_i |\delta_i(\text{TP}) - \delta_i(\text{RP})|$. For any compound C, the sums $\sum_i |\delta_i(\text{C}) - \delta_i(\text{TP})|$ and $217.9^\circ - \sum_i |\delta_i(\text{C}) - \delta_i(\text{SP})|$ should be the same if a Berry coordinate is followed for the structural distortions. The same expressions hold for the RP representation with the replacement of 217.9° by 217.7°. A plot of one sum vs. the other is shown in Figure 7.

The percent displacement along the Berry coordinate is given at the bottom of the column for each derivative in Table III. This value serves as a quantitative measure of the structural distortion. When viewed relative to the values of θ_{15} and θ_{24} for a specific substance (Table II), the principal features of the structural distortion are readily visualized.

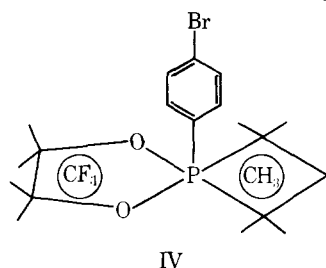
If we calculate dihedral angle differences relative to the 30° TR idealized representation $\sum_i |\delta_i(\text{C}) - \delta_i(30^\circ \text{TR})|$ from the data in Table III and subtract this difference for each compound from $T = 223.8^\circ$ (the sum of dihedral angle changes

drogen bonding, etc., will be relieved most readily by angular slippage to produce a minimum energy conformational balance. This balance will result as a compromise primarily between a tendency to reduce intramolecular energy terms (and to a lesser extent intermolecular energy terms) at the expense of moving toward the inherently higher energy associated with reaching the SP (RP) conformation. Thus, instead of seeking a structural minimum by deformations around a central atom involving more rigid bond angles (comparable in size), as appears to be the case with most compounds having coordination numbers 2, 3, 4, and 6, added flexibility is available in these cyclic phosphoranes by following a low energy bending coordinate to bring about a conformation which minimizes interactions and does so without appreciable deviation from the Berry coordinate. To do so would be more costly in energy.

We establish that this is the case by performing calculations based on conformational minimization techniques.¹¹ By allowing the Berry coordinate to be traversed with little energy input, quantitative assessment results in a minimum energy conformation, for example, for derivative 13 (Figure 4), which agrees closely with the observed^{6b} structure.

Structural Basis for Distortions. In general, movement along the Berry coordinate from the TP to the SP for the phosphoranes shown in Figure 4 (the SP becomes progressively more favored from structure 1 to 16) appears to correlate with increasing cyclization (cf. 2, 3, and 15), especially with unsaturated rings,¹ and with decreasing electronegativity of the ligand regarded as the pivotal ligand which connects the idealized TP and SP for each structure.^{1,29} In addition, the preference of the more electronegative ligands for axial sites of a TP is apparent.³⁰

In derivative 8, an interesting situation arises. Owing to the cyclic construction, the less electronegative nitrogen atom is found at an apical position of the TP shown in Figure 4. This undesirable situation leads to considerable movement toward the SP. Although structure 16 has one ring with carbon atoms attached to phosphorus, movement away from the SP is inhibited by the resulting undesirable introduction of a ring carbon having residual axial character in a TP. Actually, the related derivative IV³¹ having saturated rings, but a more



highly strained four-membered ring, is estimated to be close to 13 in location along the Berry coordinate.

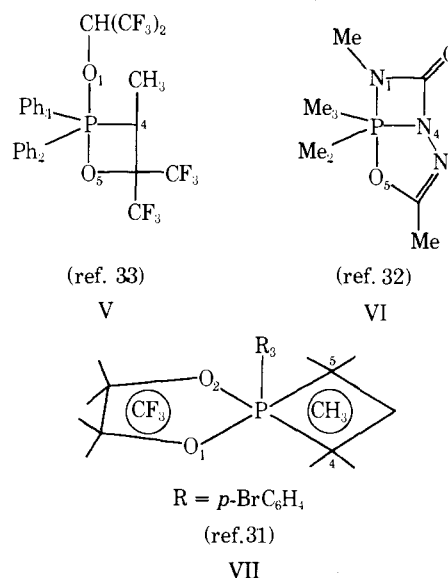
Four-Membered Ring Systems. We have estimated the distortions in three four-membered ring phosphoranes,³¹⁻³³ V, VI, and VII, according to the dihedral angle method. These values are listed in Table IV and show distortions similar to derivatives 5 and 13 of Table III. Structures VI and VII are seen to be somewhat displaced from the Berry coordinate. The major portion of the deviations is no doubt associated with the strained angles at phosphorus in the four-membered ring systems.

P-O Bond Distance Variations. All of the structures included in Figure 4 have one or more P-O bonds, except 12. The most prevalent type of P-O bond in these derivatives is present in an unsaturated five-membered ring. Since the angle variations indicate structural distortions along a Berry coordinate, corresponding evidence should exist in bond distance variations. A graph of P-O bond distances vs. the dihedral angle function, $\sum_i |\delta_i(\text{C}) - \delta_i(\text{TP})|$ (cf. Table III), for each phos-

Table IV. Dihedral Angles (δ) for Cyclic Phosphoranes with Four-Membered Rings, deg^a

δ	Structure		
	V	VI	VII
1	107.0	112.6	111.5
2	102.3	102.3	116.8
3	110.1	109.0	114.0
4	110.6	100.1	123.9
5	96.0	93.4	81.3
6	90.6	99.4	80.7
7	69.3	76.4	69.9
8	52.7	40.3	75.5
9	40.8	38.1	5.8
$\sum_i \delta_i(\text{C}) - \delta_i(\text{TP}) $	61.1	82.1	187.7
$\sum_i \delta_i(\text{C}) - \delta_i(\text{SP}) $	159.4	164.2	41.0
$S - \sum_i \delta_i(\text{C}) - \delta_i(\text{SP}) $	58.5	53.7	176.7
% along Berry coord(av)	27.5	31.2	83.7

^a See footnotes to Table III.



phorane is given in Figure 8. A list of pertinent P-O bond distances is summarized in Table V.

The variations displayed for P-O bond distances are entirely consistent with structural distortions along the TP-SP (RP) pathway. As the structural type comes closer to the idealized SP (RP), a convergence in P-O bond lengths occurs. Ring P-O bonds, which either have predominantly axial or equatorial character at the beginning of the series (Figure 4) and, consequently, a large disparity in bond distances, move to intermediate values as both types of bonds assume predominant basal character of the RP toward the end of the series. The range of values expected for P-O bonds in TP and SP (RP) geometries agrees with that calculated in an earlier study (refer to columns A and F of Table II in ref 1 and accompanying discussion).

There is an insufficient range of data to make similar plots for other types of P-O bonds. It should, however, be noted that axial P-O bond distances in saturated five-membered rings (as in derivative 5) are about 0.05 Å less than in unsaturated rings and axial P-O bond distances in acyclic substituents, about 0.1 Å less (as in derivatives 2 and 3) for compounds that are near TP in character. This indicates reduced strain in the five-membered saturated ring.¹ In accordance with this view, axial P-O bond distances in structures having four-membered rings, where ring strain should be enhanced, lie above the line in Figure 8 (cf. entries in Table IV). Hence, they are longer

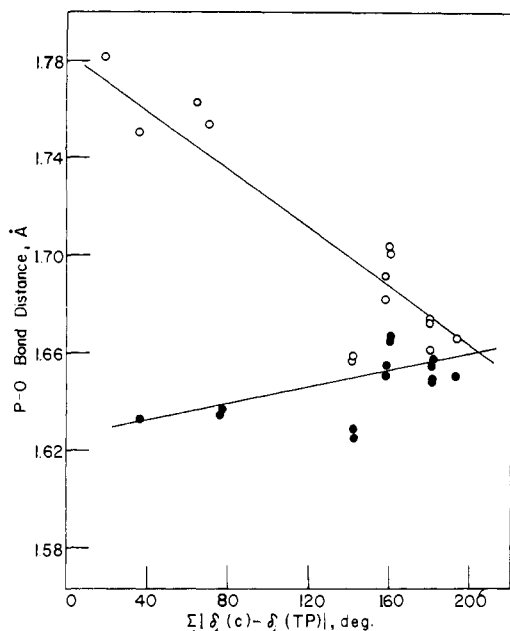


Figure 8. Variation of axial (upper line) and equatorial (lower line) P-O bond distances as structural distortion for five-membered unsaturated cyclic phosphoranes, measured by the dihedral angle sum $\sum |\delta_i(\text{C}) - \delta_i(\text{TP})|$, proceeds along the TP-SP (RP) coordinate. The solid lines are least-squares lines excluding entry 9.

than those in comparable five-membered rings. The relative strain effects in these rings in the TP and SP structures have been correlated^{1,7} with variations in P-O π bonding and substituent electronegativity. Calculations¹ show that, owing to the equal character of basal bonds in a SP, ring strain is relaxed relative to the positioning of small-membered rings, especially unsaturated ones, in an axial-equatorial orientation of a TP having unequal bond character.

Mechanistic Implications. Intramolecular Exchange Phenomena. In accounting for temperature dependent NMR data indicating the onset of a variety of intramolecular ligand interchanges in a wide assortment of trigonal bipyramidal phosphorus compounds,² successive pseudorotations (Berry processes) have been invoked to reach proposed higher energy trigonal bipyramidal exchange intermediates. With the use of topological diagrams^{34,35} the minimum number of coupled axial-equatorial bending motions required to reach the high energy intermediate may easily be determined, if not otherwise obvious. The close correspondence with the Berry coordinate for cyclic phosphoranes demonstrated here reinforces the operation of the Berry process for describing observed nonrigid behavior of phosphoranes. Accordingly, it appears likely that additional Berry processes occur, as postulated, to reach higher energy TP intermediates, but that these proposed intermediates may not be barrier states.

As an example, consider the isomerization route following a pseudorotational pathway for the adduct of dimethylphen-

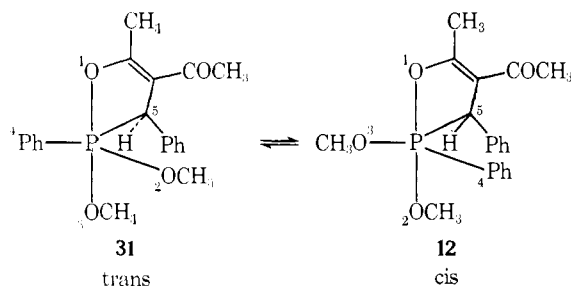
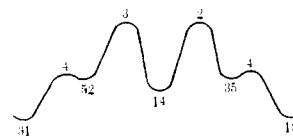


Table V. Phosphorus-Oxygen Bond Distances in Cyclic Phosphoranes, Å

Entry ^a	$\sum \delta_i(\text{C}) - \delta_i(\text{TP}) $ ^b	P-O _{ax} (ring size ^c)	P-O _{eq} (ring size ^c)
1	18.2	1.786(5) 1.737(6)	
2	34.5	1.662 1.663	1.602 1.596 1.600
3	35.4	1.751(5) 1.638	1.633(5) 1.574 1.588
4 ^d	58.5	1.715(5) 1.737(5)	
5	60.3	1.709(5) 1.709(5)	
V	61.1	1.71 1.79(4)	
6	63.7	1.700(5) 1.763(5)	
7	70.0	1.627(6) 1.754(5)	1.601(6) 1.590(6)
8	76.2	1.654(5)	1.595(5) 1.635(5) 1.637(5)
VI	82.1	1.798(5)	
9	141.1	1.659(5) 1.658(5)	1.629(5) 1.625(5)
10	157.1	1.691(5) 1.682(5)	1.650(5) 1.655(5)
11	159.0	1.701(5) 1.703(5)	1.665(5) 1.667(5)
13	179.6	1.661(5) 1.674(5)	1.658(5) 1.650(5)
14	179.5	1.672(5) 1.674(5)	1.654(5) 1.649(5)
VII	187.7	1.74(5)	1.68(5)
15	191.8	1.666(5) 1.666(5)	1.666(5) 1.650(5) 1.597

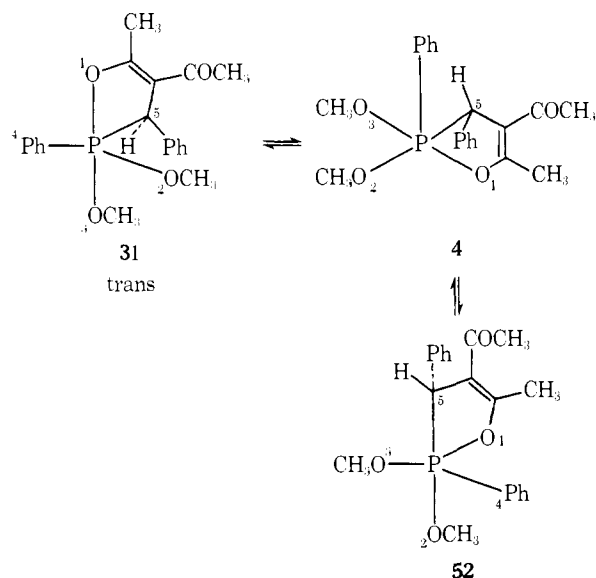
^a Identified in Figure 4 or Table IV. ^b Structural distortion as measured by the sum of the dihedral angle differences relative to the idealized TP. These values are reported in Table III. ^c The symbols following the P-O bond distance values (references as reported in Figure 4 and under the structural formulas for V to VII) have the following meaning. The number in parentheses gives the ring size. A bar over the number indicates that the ring is unsaturated. If no number is given, the directly bonded ligand is acyclic. ^d The P-O bonds for entry 4 are not part of a similar ring system as other unsaturated five-membered rings considered here since the point of unsaturation is two bonds removed from the oxygen ligand. Hence, the P-O distances are most likely between values appropriate for a saturated and unsaturated five-membered ring.

ylphosphonite and benzylideneacetylacetone.^{35,36} For this process, which requires four successive Berry pseudorotations, we envision a potential energy description of the type



where none of the levels are equal in energy. The number pairs in this topological representation (see ref 35) refer to axial positions of the TP and the single numbers refer to the apical ligand of the SP transition states. In related isomer pairs, 52 and 35, 4 and 4, 3 and 2, the phenyl group attached to the ring carbon atom is oriented differently relative to the other ligands. Consequently each member of the pair should differ slightly in energy from the other.

The initial ground state structure (31) should be near the TP end of the scale (perhaps near the structure of compound 4 of Figure 4). The first pseudorotation (31 → 52) must nec-

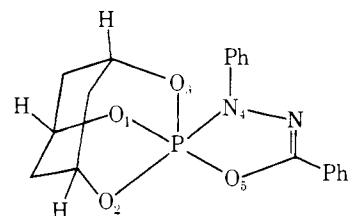


essarily pass through a SP (4) having equal trans basal angles. We regard a point at or near this representation as having maximum ligand interaction and hence, a high energy formulation. The ligand exchanged intermediate (52) probably is considerably further along the TP-SP coordinate toward SP than 31 due to the unfavorable apical orientation of a carbon atom (operation of the electronegativity rule).^{30b} Thus, the distortion produces a better balance of ligand interactions and the full apical character of the ring carbon is not realized. These factors should lead to a lower energy relative to the conformation discussed for 4.

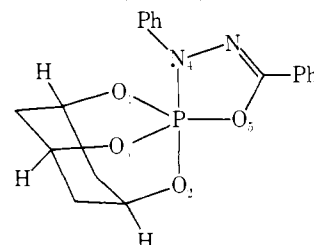
Each successive pseudorotation should be similar, the relative energy governed by the relative isomer energy gauged by substituent axiophilicities, ring constraints, and steric factors. Thus, 3 is shown higher than 4 because a less electronegative group is present in the axial position of the SP (4) relative to 3.²⁹ Isomer 14 should not be nearly as distorted from the TP compared to 52 because a more electronegative phenyl group has apical character instead of a ring carbon atom. Hence, isomer 14 should have a lower energy than 52. The isomerization process indicated by NMR data^{35,36} is completed by two more pseudorotations completely analogous to the first two discussed above.

Structure 8 of Figure 4 is interesting in this regard. Were it not for the bicyclic nature of the tridentate ligand, the nitrogen atom would preferentially position itself equatorially in a near TP frame. As it is, the ring constraints tend to place the bridgehead nitrogen atom toward an apical position of the TP and the more electronegative ring oxygen equatorial. To counter this tendency, the ring system achieves better stability by becoming more planar as the structure distorts toward a SP. As a consequence, the ground state structure is found near the halfway point of the TP-SP coordinate (Figure 7). This gives us some idea of the distortion expected for isomer 52. The fact that the distortion of structure 8 is along the Berry pathway, in spite of its forced configuration, gives added credence to the operation of pseudorotations involving high-energy intermediates.

The adamantanoid derivative 7 and related substances show rapid positional exchange¹⁶ on the NMR time scale. As indicated in Figure 4, the structure of 7 is approximately 30% displaced (Table III) along the Berry coordinate toward the SP. This SP, which is a most likely representation of the



transition state for ligand exchange in 7, is easily reached by the axial-equatorial bending combination of the Berry process since the ground state TP is already considerably displaced toward this formation. Continuation of the bending action yields the intermediate TP, which, when followed by a second



pseudorotation (P-O₁ is the pivotal bond) through a SP transition state similar to that above, completes the basic exchange mechanism.

Acknowledgment. This investigation was supported by grants from the National Science Foundation (MPS 74-11496) and from the National Institutes of Health (GM 21466), which are gratefully acknowledged. We are also grateful to the University of Massachusetts Computer Center for generous allocation of computer time.

References and Notes

- (1) Pentacoordinated Molecules. 21. Previous paper in this series: R. R. Holmes, *J. Am. Chem. Soc.*, **97**, 5379 (1975).
- (2) Extensive reviews of the NMR data are found in the following sources: (a) R. Lukenbach, "Dynamic Stereochemistry of Pentacoordinated Phosphorus and Related Elements", George Thieme Verlag, Stuttgart, 1973; (b) D. Hellwinkel, "Organo Phosphorus Compounds", Vol. 3, G. M. Kosolapoff and L. Maier, Ed., Wiley-Interscience, New York, N.Y., 1972, p 185.
- (3) R. S. Berry, *J. Chem. Phys.*, **32**, 933 (1960).
- (4) D. Z. Denney, D. W. White, and D. B. Denney, *J. Am. Chem. Soc.*, **93**, 2066 (1971).
- (5) (a) P. Gillespie, P. Hoffmann, H. Klusacek, D. Marquarding, S. Pfohl, F. Ramirez, E. A. Tsolis, and I. Ugi, *Angew. Chem., Int. Ed. Engl.*, **10**, 687 (1971); (b) F. Ramirez and I. Ugi, *Adv. Phys. Org. Chem.*, **9**, 256 (1971); (c) I. Ugi, F. Ramirez, D. Marquarding, H. Klusacek, and P. Gillespie, *Acc. Chem. Res.*, **4**, 288 (1971); (d) F. Ramirez and I. Ugi, *Bull. Soc. Chim. Fr.*, 453 (1974).
- (6) (a) H. Wunderlich, D. Mootz, R. Schmutzler, and M. Wieber, *Z. Naturforsch. B*, **29**, 32 (1974); (b) H. Wunderlich, *Acta Crystallogr., Sect. B*, **30**, 939 (1974); (c) H. Wunderlich and D. Mootz, *ibid.*, **30**, 935 (1974).
- (7) R. R. Holmes, *J. Am. Chem. Soc.*, **96**, 4143 (1974).
- (8) E. L. Muetterties and L. J. Guggenberger, *J. Am. Chem. Soc.*, **96**, 1748 (1974).
- (9) (a) R. K. Brown and R. R. Holmes, *J. Am. Chem. Soc.*, **99**, 3326 (1977); (b) P. F. Meunier, J. A. Deiters, and R. R. Holmes, *Inorg. Chem.*, **15**, 2572 (1976); (c) P. F. Meunier, J. R. Devillers, and R. R. Holmes, work submitted for publication.
- (10) J. R. Devillers and R. R. Holmes, *J. Am. Chem. Soc.*, **99**, 3332 (1977).
- (11) J. A. Deiters, J. C. Gallucci, T. E. Clark, and R. R. Holmes, work submitted for publication.
- (12) R. Sarma, F. Ramirez, and J. F. Maracek, *J. Org. Chem.*, **41**, 473 (1976).
- (13) D. D. Swank, C. N. Caughlan, F. Ramirez, and J. F. Pilot, *J. Am. Chem. Soc.*, **93**, 5236 (1971).
- (14) R. Sarma, F. Ramirez, B. McKeever, J. F. Maracek, and S. Lee, *J. Am. Chem. Soc.*, **98**, 581 (1976).
- (15) (a) W. C. Hamilton, S. J. LaPlaca, and F. Ramirez, *J. Am. Chem. Soc.*, **87**, 127 (1965); (b) R. D. Spratley, W. C. Hamilton, and J. Ladell, *ibid.*, **89**, 2272 (1967).
- (16) (a) W. C. Hamilton, J. S. Ricci, Jr., F. Ramirez, L. Kramer, and P. Stern, *J. Am. Chem. Soc.*, **95**, 6335 (1973); (b) H. L. Carrell, H. M. Berman, J. S. Ricci, Jr., W. C. Hamilton, F. Ramirez, J. F. Maracek, L. Kramer, and I. Ugi, *ibid.*, **97**, 38 (1975).
- (17) D. Hellwinkel, W. Krapp, D. Schomburg, and W. S. Sheldrick, *Z. Naturforsch. B*, **31**, 948 (1976).
- (18) (a) W. S. Sheldrick, A. Schmidpeter, and J. H. Weinmaier, *Angew. Chem.*, **87**, 519 (1975); (b) W. S. Sheldrick, *Acta Crystallogr., Sect. B*, **32**, 925 (1976).
- (19) W. S. Sheldrick, personal communication; A. Schmidpeter, D. Schomburg, W. S. Sheldrick, and J. H. Weinmaier, *Angew. Chem.*, **88**, 851 (1976).

- (20) W. S. Sheldrick, personal communication.
- (21) M. Eisenhut, R. Schmutzler, and W. S. Sheldrick, *J. Chem. Soc., Chem. Commun.*, 144 (1973), and personal communication.
- (22) This column is simply obtained by noting which observed angles fall outside the range of the values of the respective angles traversed between the idealized TP and SP (RP) structures (Figure 3), measuring the number of degrees that each fall outside the range, taking their sum, and multiplying by two.
- (23) Nine dihedral angles are given based on the idealized TP geometry in Figure 3(a). Additional dihedral angles arise for actual structures but are not common to the idealized structures being used for comparison.
- (24) (a) A. Rauk, L. C. Allen, and K. Mislow, *J. Am. Chem. Soc.*, **94**, 3035 (1972); (b) R. Hoffmann, J. M. Howell, and E. L. Muetterties, *ibid.*, **94**, 3047 (1972); (c) L. S. Bartell and V. Plato, *ibid.*, **95**, 3097 (1973); (d) A. Strich and A. Veillard, *ibid.*, **95**, 5574 (1973).
- (25) (a) R. R. Holmes, *Acc. Chem. Res.*, **5**, 296 (1972); (b) R. R. Holmes, L. S. Couch, and C. J. Hora, Jr., *J. Chem. Soc., Chem. Commun.*, 197 (1974).
- (26) L. S. Bernstein, J. J. Kim, K. S. Pitzer, S. Abramowitz, and I. Levin, 30th Symposium on Molecular Structure and Spectroscopy. The Ohio State University, Columbus, Ohio, June 1975, Abstract No. TA6; L. S. Bernstein, S. Abramowitz, and I. W. Levin, *J. Chem. Phys.*, **64**, 3228 (1976); L. S. Bernstein, J. J. Kim, K. S. Pitzer, S. Abramowitz, and I. W. Levin, *ibid.*, **62**, 3671 (1975).
- (27) (a) L. S. Bartell, *Inorg. Chem.*, **9**, 1594 (1970); (b) K. W. Hansen and L. S. Bartell, *ibid.*, **4**, 1775 (1965); (c) L. S. Bartell and K. W. Hansen, *ibid.*, **4**, 1777 (1965); (d) F. B. Clippard, Jr., and L. S. Bartell, *ibid.*, **9**, 805 (1970); (e) W. J. Adams and L. S. Bartell, *J. Mol. Struct.*, **8**, 23 (1971); (f) H. Yow and L. S. Bartell, *ibid.*, **15**, 209 (1973).
- (28) (a) J. E. Griffiths, R. P. Carter, Jr., and R. R. Holmes, *J. Chem. Phys.*, **41**, 863 (1964); (b) I. W. Levin, *ibid.*, **50**, 1031 (1969); (c) F. A. Miller and R. J. Capwell, *Spectrochim. Acta, Part A*, **27**, 125 (1971); (d) I. W. Levin, *J. Mol. Spectrosc.*, **33**, 61 (1970).
- (29) As previously cited^{7,25a} electron-pair repulsion considerations, with reference to the idealized SP in Figure 3(b), suggest a correspondence in bond properties between the basal bonds of the SP and axial bonds of the TP. Thus, the more electronegative ligands would prefer the basal positions of the SP and small-membered rings would locate in a *cis-basal* rather than a basal-axial pair. The latter correspondence for the SP follows from the element and strain rules for the TP.³⁰
- (30) (a) F. H. Westheimer, *Acc. Chem. Res.*, **1**, 70 (1968); (b) E. L. Muetterties, W. Mahler, and R. Schmutzler, *Inorg. Chem.*, **2**, 613 (1963); (c) E. L. Muetterties, W. Mahler, K. J. Packer, and R. Schmutzler, *ibid.*, **3**, 1298 (1964).
- (31) J. A. Howard, D. R. Russell, and S. Trippett, *J. Chem. Soc., Chem. Commun.*, 856 (1973).
- (32) A. Schmidpeter, J. Luber, D. Schomburg, and W. S. Sheldrick, *Chem. Ber.*, in press.
- (33) M.-Ul-Haque, C. N. Caughlan, F. Ramirez, J. F. Pilot, and C. P. Smith, *J. Am. Chem. Soc.*, **93**, 5229 (1971).
- (34) K. Mislow, *Acc. Chem. Res.*, **3**, 321 (1970).
- (35) (a) D. Gorenstein and F. H. Westheimer, *J. Am. Chem. Soc.*, **92**, 634 (1970); (b) D. Gorenstein, *ibid.*, **92**, 644 (1970).
- (36) F. Ramirez, *Acc. Chem. Res.*, **1**, 168 (1968).

The Crystal and Molecular Structure of the Spirophosphorane (C₆H₄O₂)₂PC₆H₅¹

Richard K. Brown² and Robert R. Holmes*

Contribution from the Department of Chemistry, University of Massachusetts, Amherst, Massachusetts 01003. Received September 20, 1976

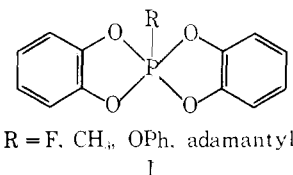
Abstract: The crystal structure of 2-phenyl-2,2'-spirobis(1,3,2-benzodioxaphosphole). (C₆H₄O₂)₂PC₆H₅, has been determined by single crystal x-ray diffraction analysis. The compound crystallizes in the monoclinic space group *P2₁/c* with cell constants *a* = 6.663 (7), *b* = 17.182 (6), *c* = 13.301 (5) Å, β = 88.78 (7)°, *Z* = 4. It has a noncrystallographic twofold axis. The geometry about phosphorus is near rectangular pyramidal (RP). The structural deviations from an idealized RP are along the Berry ligand exchange coordinate. Pertinent features of the molecule are the diagonal O-P-O angles, 160.0 (2) and 145.4 (2)°, and the four bond angles between the axial phenyl group and the basal P-O bonds, 108.5 (2), 100.0 (2), 100.0 (2), 106.1 (2)°. The differences in the basal P-O bond lengths, 1.650 (4) and 1.655 (4) vs. 1.682 (4) and 1.691 (4) Å, are indicative of a small residual trigonal bipyramidal character. The phosphorus atom is 0.39 Å out of the mean plane of the four oxygen atoms toward the axial phenyl group.

The structures of cyclic phosphoranes are especially interesting because they serve as models for transition states in many reaction mechanisms of four-coordinate phosphorus.³ For example, the mode of hydrolysis of cyclic phosphates^{3,4} and phosphonium salts,³ the enzymatic cleavage of ribonucleic acids by ribonucleases,⁵ and the chain elongation mechanism of DNA and RNA replication⁶ depend intimately on the detailed structural principles developed from studies on isolatable phosphoranes.

It has recently become apparent⁷ that most structural distortions of cyclic phosphoranes can be understood in terms of low angle bending force constants associated with the Berry coordinate⁸ governing intramolecular ligand exchange^{3a} and that the appearance of structures at specific points along the coordinate is primarily determined by a competition between factors resulting from the ligand construction which influence the energy difference between the idealized trigonal bipyramidal (TP) and square or rectangular pyramidal SP (RP) framework.

An intimate knowledge of the steric and electronic factors which determine the extent of structural glide along the TP-SP (RP) pathway is needed to quantitatively assess the structural makeup of proposed transition states and their influence in establishing specific reaction mechanisms.

Spirophosphoranes containing two catechol residues and a variety of different ligands in the fifth position offer a suitable series on which to test postulates concerning molecular properties leading to the stabilization of the SP (RP) geometry.⁹ Previously studied members I have structures¹⁰⁻¹² which fall toward the idealized RP form.



The presence of a phenyl group at the fifth position offers the interesting possibility of ascertaining the influence of going from an sp³ to an sp² type carbon atom as well as judging the influence of comparative steric effects of the phenyl and phenoxy groups on the catechol ring system.

Experimental Section

Preparation. Samples of 2-phenyl-2,2'-spirobis(1,3,2-benzodioxaphosphole) were prepared by the direct interaction of 2 molar equiv of catechol in ether with 1 molar equiv of dichlorophenylphosphine at ambient temperature for 1 h.¹³ Removal of the solvent resulted in